doi:10.1016/j.jmb.2010.11.051 J. Mol. Biol. (2011) 406, 205–214

Contents lists available at www.sciencedirect.com

Journal of Molecular Biology

journal homepage: http://ees.elsevier.com.jmb

COMMUNICATION

HIV-1 Gag Extension: Conformational Changes Require Simultaneous Interaction with Membrane and Nucleic Acid

Siddhartha A. K. Datta[1], Frank Heinrich[2], Sindhu Raghunandan[3], Susan Krueger[3], Joseph E. Curtis[3], Alan Rein[1] and Hirsh Nanda[3]*

[1]*HIV Drug Resistance Program, National Cancer Institute, P.O. Box B, Building 535, Fredrick, MD 21702-1201, USA*
[2]*Department of Physics, Carnegie Mellon University, 5000 Forbes Avenue, Pittsburgh, PA 15213-3890, USA*
[3]*NIST Center for Neutron Research, National Institute of Standards and Technology, 100 Bureau Drive, Gaithersburg, MD 20899-6102, USA*

Received 27 September 2010; received in revised form 24 November 2010; accepted 25 November 2010
Available online 4 December 2010

Edited by R. Huber

Keywords:
retroviral assembly;
neutron reflectivity;
SANS;
disordered proteins;
tethered membranes

The retroviral Gag polyprotein mediates viral assembly. The Gag protein has been shown to interact with other Gag proteins, with the viral RNA, and with the cell membrane during the assembly process. Intrinsically disordered regions linking ordered domains make characterization of the protein structure difficult. Through small-angle scattering and molecular modeling, we have previously shown that monomeric human immunodeficiency virus type 1 (HIV-1) Gag protein in solution adopts compact conformations. However, cryo-electron microscopic analysis of immature virions shows that in these particles, HIV-1 Gag protein molecules are rod shaped. These differing results imply that large changes in Gag conformation are possible and may be required for viral formation. By recapitulating key interactions in the assembly process and characterizing the Gag protein using neutron scattering, we have identified interactions capable of reversibly extending the Gag protein. In addition, we demonstrate advanced applications of neutron reflectivity in resolving Gag conformations on a membrane. Several kinds of evidence show that basic residues found on the distal N- and C-terminal domains enable both ends of Gag to bind to either membranes or nucleic acid. These results, together with other published observations, suggest that simultaneous interactions of an HIV-1 Gag molecule with all three components (protein, nucleic acid, and membrane) are required for full extension of the protein.

**Corresponding author*. NIST Center for Neutron Research, National Institute of Standards and Technology, 100 Bureau Drive, Stop 6103, Gaithersburg, MD 20899-6103, USA. E-mail address: hirsh.nanda@nist.gov.

Abbreviations used: HIV-1, human immunodeficiency virus type 1; MA, matrix; CA, capsid; NC, nucleocapsid; NA, nucleic acid; WT, wild type; VLP, virus-like particle; SANS, small-angle neutron scattering; EM, electron microscopy; ssDNA, single-stranded DNA; tBLM, tethered bilayer lipid membrane; NR, neutron reflectivity; nSLD, neutron scattering length density.

0022-2836/$ - see front matter. Published by Elsevier Ltd.

Introduction

Expression of a single retroviral protein, termed Gag, is sufficient for virus particle formation in mammalian cells.[1,2] Gag is a multi-domain protein always containing, from N- to C-terminus, a matrix (MA) domain, a capsid (CA) domain, and a nucleocapsid (NC) domain. The particles assembled from Gag are immature virions; in most retroviruses, including lentiviruses such as human immunodeficiency virus type 1 (HIV-1), these particles form as Gag accumulates at the cytoplasmic face of the plasma membrane. Targeting of Gag to the plasma membrane is a function of the MA domain and involves, on the one hand, an electrostatic interaction between basic residues in MA and anionic lipids in the membrane and, on the other hand, a hydrophobic interaction between membrane lipids and myristic acid, a 14-carbon saturated fatty acid at the extreme N-terminus of the protein.[3] The protein–protein interactions leading to virus assembly are largely or exclusively a function of the CA domain, while the NC domain plays a principal role in the interactions of Gag with nucleic acids (NAs).

Immature retrovirus particles are roughly spherical, with an average diameter of around 1100 Å. The Gag proteins in these particles are extended rods, approximately 200 Å long.[4] They are arranged as radii of the particles, with their N-termini in contact with the lipid bilayer that surrounds the particle and their C-termini projecting into the interior of the particle, presumably in contact with RNA. A transmission electron micrograph of these particles, budding from the plasma membrane of a mammalian cell, is shown in Fig. 1a.

We have previously characterized the properties of recombinant HIV-1 Gag protein, purified from bacteria.[7] This protein differs from authentic, wild-type (WT) HIV-1 Gag protein in lacking both the myristic acid modification at its N-terminus and a domain at the extreme C-terminus termed p6. When NA is added, this protein assembles into virus-like particles (VLPs); however, these VLPs are far smaller than authentic retrovirus particles, with a diameter of only 250 Å to 300 Å.[5] Figure 1b shows examples of the small VLPs formed with NA alone. These VLPs are too small to be composed of 200-Å rods of Gag. In fact, the shell of protein forming these VLPs appears to be only 70 Å to 80 Å thick. However, correctly sized VLPs are assembled if inositol pentakisphosphate as well as NA is added to purified Gag.[9] The striking difference between the particles in Fig. 1a and b implies that HIV-1 Gag can adopt alternative conformations, one extended (forming authentic particles) and one bent (as in the VLPs in Fig. 1b).

This conformational freedom presumably reflects the flexibility of the linker regions between the domains in the Gag polyprotein. Solution-state NMR demonstrated the MA and CA domains to be rotationally uncoupled by a 26-amino-acid linker.[10] Structural determination of the CA domain by crystallography revealed five disordered residues linking separate N-terminal and C-terminal domains.[11] Furthermore, NC, p6, and p2 domains appear to be largely unstructured, except for the Zn-finger regions within NC.[12–15] Difficulties in characterizing intrinsically disordered domains have led to a lack of high-resolution information for the intact Gag protein.

In previous investigations, structural properties of recombinant Gag protein in solution were probed using hydrodynamic data and small-angle neutron scattering (SANS) together with molecular modeling.[7] This study used a Gag mutant (designated WM Gag) that was inhibited from dimerizing. The results indicated that the protein is compact in solution, with its terminal domains situated close in three-dimensional space. It seems likely that the protein monomer in solution actually adopts an ensemble of interconverting, relatively compact structures.

In authentic immature particles, each Gag molecule is in contact with other Gag molecules, with the lipid bilayer surrounding the particle, and with the RNA within the particle. The question then arises as to which of these interactions is responsible for the extension of the Gag protein in these particles. In the present work, we have explored the conditions under which HIV-1 Gag protein is compact, as it is in free solution and small VLPs, or extended, as it is in immature virions. We used neutron scattering methods to dissect the contributions of protein–protein, protein–lipid, and protein–NA interactions to the extension of the protein.

Protein–protein interactions

HIV-1 Gag exists in solution in monomer–dimer equilibrium.[6] The interface mediating the dimeric interaction is in the C-terminal portion of the CA domain. In order to determine whether dimerization leads to extension of the WT protein, we used SANS to measure the mean scattering particle size or radius of gyration, R_g, of WT Gag over a broad concentration range. Results of this experiment are shown in Fig. 1c. The figure shows the R_g data (left axis) for WT Gag and WM Gag as a function of protein concentration; for the WT Gag, the fraction of protein present in dimers is depicted with a blue broken line and was calculated using a K_d of 3.9 μM in D_2O buffer.[6]

As shown in Fig. 1c, the R_g of the WT Gag protein increased as the dimeric fraction increased. At low concentration (0.25 mg/ml, or 5 μM), where 55% of the molecules are in dimers, the weight-averaged R_g is 38 Å, slightly larger than the monomeric Gag value of 35 Å. As the protein concentration increases, the

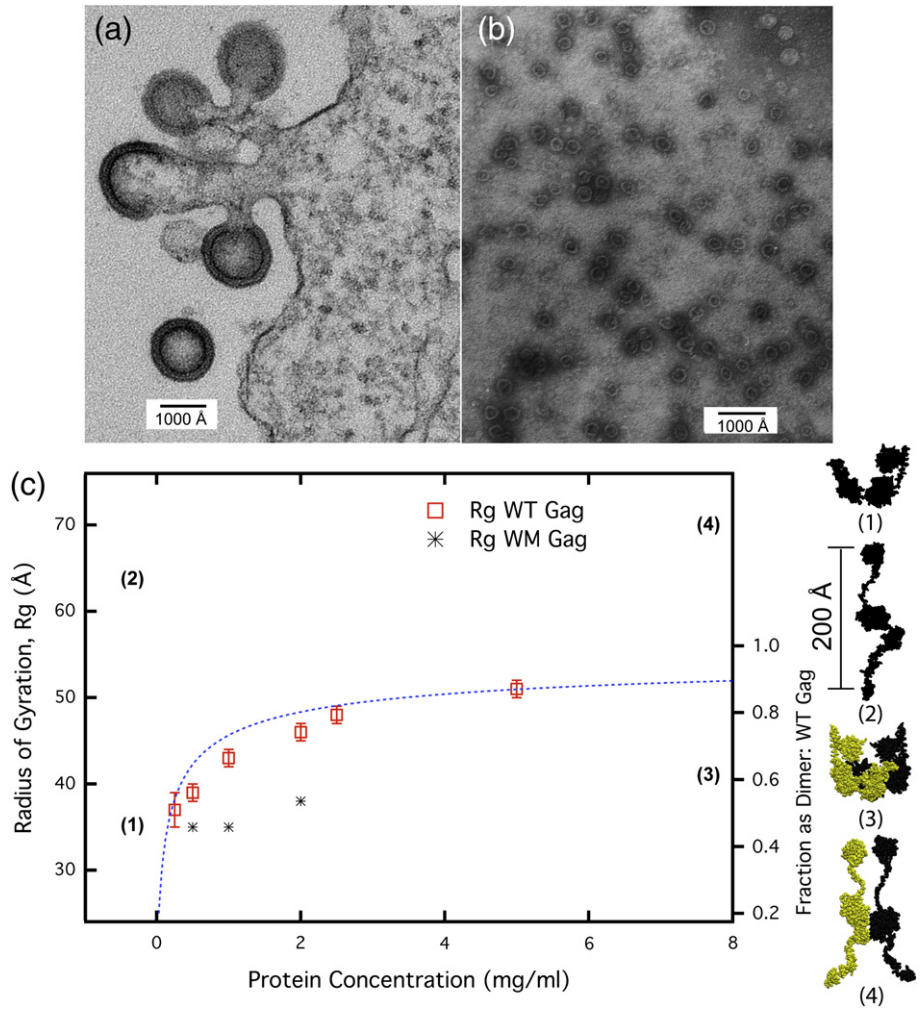

Fig. 1. Gag dimensions. (a) Gag assembly at different stages of immature virion formation imaged by EM as described in Supplementary Methods. Protein shell in both the spherical virion and incomplete arcs has a thickness of ≈200 Å. (b) Recombinant HIV Gag VLPs assembled *in vitro* with yeast tRNA under standard conditions[5] (described in Supplementary Methods) at physiological salt buffers and visualized by negative-stain EM. These VLPs have a diameter 3× smaller than that of native virions and the protein shell is only 70 Å to 80 Å in thickness. (c) Average protein size in solution as a function of protein concentration. R_g was measured by SANS for WT Gag and WM Gag. The percentage of WT Gag molecules as dimer was calculated (blue broken line) using a K_d of 3.9 μM in D_2O.[6] WM Gag has a binding constant 100× weaker than that of WT and was assumed to be pure monomer over this concentration range. Models for Gag monomer and dimers are shown on the right based on SANS results for the compact state[7] and cryo-EM data for the extended state.[4] The dimerization interface solved by solution NMR[8] for the CA domain was used as a template for generating the dimer complex. The calculated radii of gyration for both the compact/extended and monomer/dimer configurations are shown on the plot by their numerical designation: (1), monomer in solution; (2), extended monomer, as in authentic immature virions; (3), dimer of (1); (4), dimer of (2).

R_g increases, reaching a plateau at ≈50 Å; at the maximum concentrations used here (100 μM), >90% of the molecules are in dimers.

As a frame of reference, models of the compact and extended state of Gag were constructed to provide R_g limits for the monomeric and dimeric protein. The compact Gag conformations were taken from the set of representative structures determined by Datta *et al.*[7] The extended conformation was based on cryo-electron microscopy (EM) data of Fuller *et al.*[4] The cryo-EM results provided distributions of the structured Gag domains arranged radially from the membrane surface in the immature virion. Starting with the compact model, backbone dihedral conformations of the flexible linkers were varied until the cryo-EM distribution constraints were satisfied. Further details on modeling and defining the structured

and flexible regions are given in the Supplementary Material. The software program SASSIE[16] was used to perform the conformational search. Even in the extended state, multiple linker conformations were possible but the differences in R_g were <5%. Therefore, a representative structure was chosen for experimental comparison. To generate dimers, the Gag monomers were oriented with respect to each other using the dimerization interface between CA domains solved by solution NMR[8] as a reference template.

The experimental results indicate that the actual Gag dimer adopts R_g values larger than the compact dimer model but smaller than the extended dimer model. Even at concentrations where 90% of the population is in dimers, protein dimensions are not consistent with the extended dimer. Rather, dimeric Gag molecules in solution appear to adopt an ensemble of conformations that are shifted towards intermediate, partially extended configurations. Hence, protein–protein interactions are not sufficient to fully extend the Gag protein.

Protein–NA interactions

Within the immature virion, the NC domain of Gag is believed to associate with RNA. *In vitro* studies also demonstrate the importance of Gag–NA interactions, as assembly of recombinant Gag protein into VLPs can be triggered by addition of RNA or single-stranded DNA (ssDNA).[5,17,18] However, the effect of NA on Gag protein conformation has not been previously investigated. The size of recombinant Gag in the presence of ssDNA was examined using SANS. Oligodeoxynucleotides that are either 5 (TGx2.5) or 14 (TGx7) bases long with the repeating sequence $(TG)_n$ were added to Gag, as HIV-1 NC has very high affinity for this sequence.[19] Both TGx2.5 and TGx7 bind the NC domain of Gag tightly, but only TGx7 supports assembly, though relatively inefficiently and at low ionic strength.[5] Protein and DNA were incubated together in 0.5 M NaCl buffer. Under these conditions, fluorescence anisotropy assays showed that the K_d for protein–DNA binding is below 1 μM (Supplementary Fig. 2),

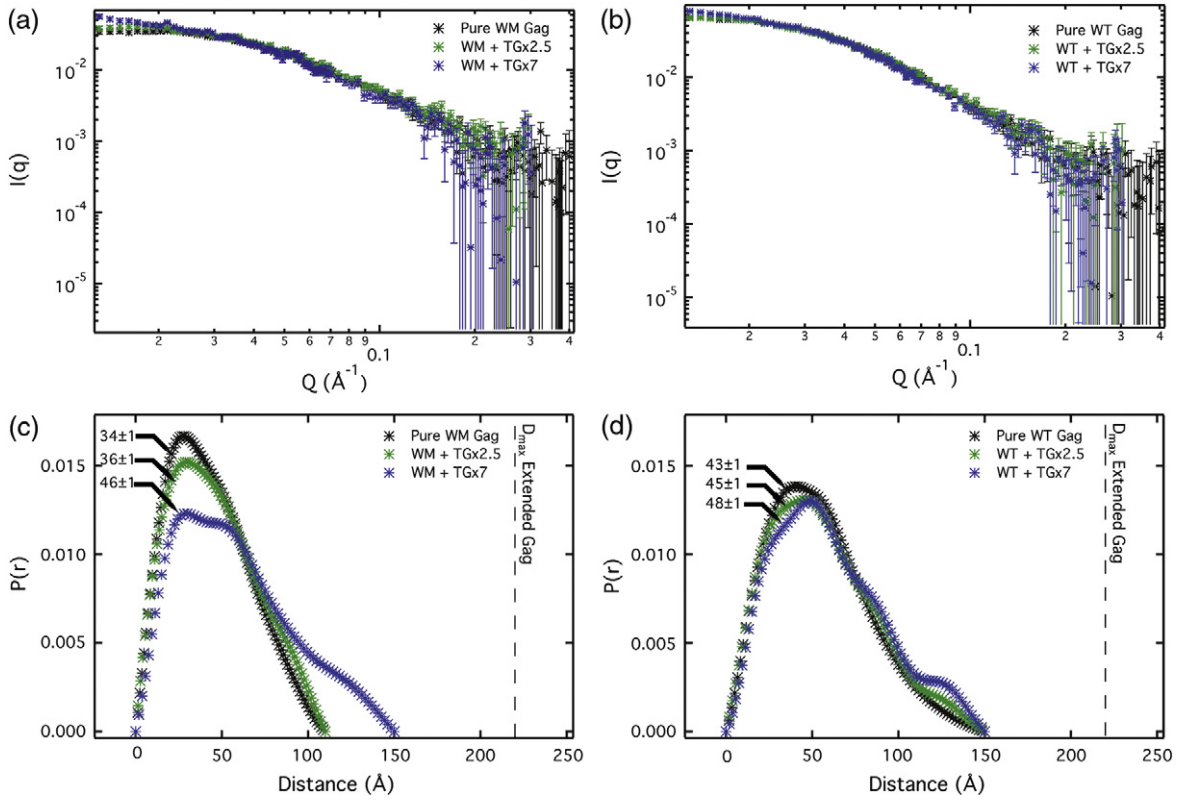

Fig. 2. The influence of ssDNA on Gag conformation. WM and WT Gag protein at 20 μM were incubated with short NA segments containing a TG base sequence repeat. Two different lengths, TGx2.5 and TGx7, were used at 240 μM and 80 μM, respectively. The SANS spectra of WM Gag and WT Gag are shown in (a) and (b). The pair-distance distribution $P(r)$ determined from the SANS data are shown in (c) and (d) with R_g values for each condition indicated on the plot. Incubation was performed at 0.5 M NaCl to inhibit protein condensation in the presence of NA. Gag–TG binding constant, K_d, was determined to be <1 μM by independent fluorescence anisotropy measurements (see Supplementary Fig. 2). Excess NA assured complete Gag binding in the SANS experiment.

but the binding does not lead to VLP assembly. SANS measurements were performed using a 4- to 12-fold excess of DNA to ensure protein saturation under these conditions.

Both WM and WT Gag were studied in order to isolate the contribution of protein–NA and protein–protein–NA interactions. The SANS profiles for WM Gag, presumably resistant to protein–protein interactions, are shown in Fig. 2a; little difference is seen between the pure protein (black) and the protein–TGx2.5 (5-base DNA) (green) mixture. The sample containing the 14-base oligodeoxynucleotide TGx7 (blue) resulted in a slight increase in scattering at low q, indicating the presence of a small population of higher-order protein oligomers. WT Gag treated similarly was nearly invariant for all protein samples (Fig. 2b). The changes in the spectra are due to alteration in protein conformation, as the NA does not contribute to the observed scattering under the contrast conditions used.

The pair-distance distribution functions, $P(r)$, shown in Fig. 2c and d were determined from the SANS profiles and provide both the mean R_g and the maximum dimensions of the protein molecules in solution. For WM Gag (Fig. 2c), the pure protein and the protein in the presence of short TGx2.5 NA had R_g values of 34 ± 1 Å and 36 ± 1 Å, respectively. The resulting molecular sizes are similar to what was found for a compact monomeric protein in solution (Fig. 1c, WM Gag). The complexes formed on TGx7 have an R_g of 46 ± 1 Å, similar to that determined for WT Gag dimers in solution (Fig. 1c). The value of D_{max} for WM Gag bound to TGx7 increases to that of WT Gag in solution. It seems plausible that the 14-base strand can bind two Gag molecules via interactions with the NC domain and thus promote Gag dimerization despite WM Gag's reduced interprotein affinity. Indeed, WM Gag is capable of assembly into small VLPs *in vitro*.[7] Similar sized complexes were found for WT Gag both as pure protein and in the presence of the TG DNA, where R_g values ranged from 43 ± 1 Å to 48 ± 1 Å. NA had little effect on molecular sizes, possibly because WT Gag dimerizes spontaneously in solution. Hence, both WM and WT Gag form similar sized complexes upon binding TGx7. However, as shown in Fig. 2c and d, the maximum dimensions observed in both cases were significantly below the expected D_{max} calculated from the extended Gag model shown in Fig. 1c. These results suggest that protein–NA interactions are also not sufficient to extend Gag.

In the presence of longer NAs such as yeast tRNA, ≈80 nucleotides in length, Gag protein readily condenses *in vitro*, forming organized structures such as those shown in Fig. 1b. These condensed VLPs present a model system for strongly coupled protein–protein–NA interactions. As discussed previously, these VLPs have a diameter and protein shell thickness indicative of a compact Gag protein. Thus, additional interactions are required for Gag protein to adopt extended conformations.

Protein–membrane interactions

HIV-1 particle assembly occurs at the inner face of the cell membrane. Therefore, the membrane itself might play an important role in protein structure. A novel system has been engineered as a cell membrane biomimetic to investigate protein structure and interaction with lipid membranes. We used a tethered bilayer lipid membrane (tBLM) system consisting of a 14-carbon lipid in which the headgroup has been replaced with a short polyethylene glycol linker terminated by a thiol group.[20] The thiol anchors the lipid tether to a gold film on a solid Si wafer substrate. The lipid tether sparsely covers the surface and nucleates the formation of a lipid membrane during a rapid solvent exchange procedure.[20,21] The resulting membrane is separated from the support by a 20 - to 30-Å, highly hydrated layer. We showed recently that the diffusivity of phospholipids in the leaflet distal to the solid support is indistinguishable from that in vesicle membranes.[22] The tBLM system by design allows us to control the conditions of protein membrane binding while performing in situ structural measurements.

Lipid membrane and protein structure in the tBLM were investigated by neutron reflectivity (NR). With the NR technique, the intensity of neutrons reflected off of thin films at increasing grazing angles is measured. At these low angles, neutrons penetrate the film surface a few thousand angstroms. Therefore, neutrons that reflect off of buried interfaces (e.g., the interface between the lipid bilayer and the Au substrate or that between the Au layer and the Cr layer of the substrate) interfere both constructively and destructively, thereby modulating the reflected intensity. The results are interpreted in terms of a one-dimensional neutron scattering length density (nSLD) profile. The nSLD profile depends on the structure and distribution of lipid groups and protein normal to the membrane plane. NR is one of the few methods that can characterize membrane protein structure in physiologically relevant conditions, that is, on a fluid lipid bilayer.

Because NR averages over the in-plane organization of molecules on the membrane surface, the nSLD profile is represented using homogenous slabs organized normal to the membrane. The thickness and neutron scattering density of each slab are dependent upon the distribution of chemical groups that the slab represents (lipid chain, lipid headgroup, protein, etc.). Analysis of NR data requires using the slab model and computing a trial reflectivity spectrum by the Parratt formalism.[23] Optimization of the slab model parameters is performed to fit the experimental reflectivity data.

The resulting nSLD profile is then interpreted in terms of the underlying biological architecture. Uncertainties in our model parameters are rigorously defined using a Monte Carlo error analysis.[24] This analysis has been implemented in a customized version of the software suite *ga_refl*,[25] provided by the National Institute of Standards and Technology Center for Neutron Research.

Gag binding was studied on a tBLM system composed of 30% anionic phosphatidylserine and 70% neutral lipids. This system has a negative charge density similar to that found in the native

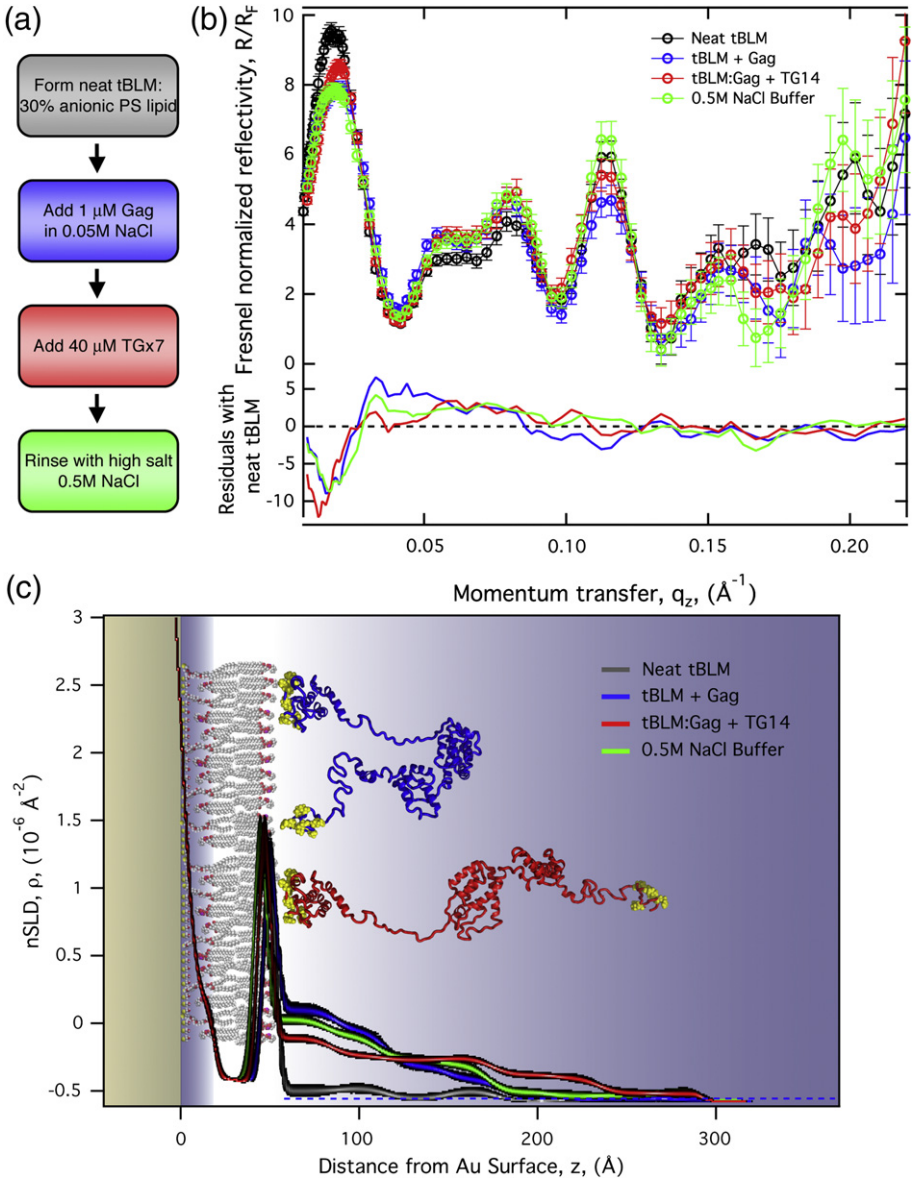

Fig. 3. NR results of WT Gag protein interacting with a tBLM indicates conditions that alter Gag conformation. (a) The sequence of measurements performed in situ on the reflectometry instrument. The steps are as follows: (1) Formation of a complete tBLM. (2) Binding WT Gag (buffer: 0.05 M NaCl, 0.001 M $NaPO_4$, and 5 mM TCEP, pH 7.4). (3) Binding of TGx7 DNA to the Gag protein layer. (4) Disassociation of TGx7 using a high-ionic-strength buffer (same as binding buffer except 0.5 M NaCl). For each experimental condition, three different isotopic aqueous buffer contrasts (mixtures of H_2O and D_2O) were used. (b) The resulting reflectivity spectra for the series of measurements showing the pure H_2O buffer data only. Differences in reflectivity from the neat tBLM condition are given as residuals in the bottom. (c) A one-dimensional nSLD profile of the membrane and Gag determined by fitting the reflectivity data to a "slab model" (see the main text for details). Line widths represent the 95% confidence limits. The insets showing WT Gag cartoons are illustrative models of protein conformations consistent with the overall dimensions determined by reflectivity.

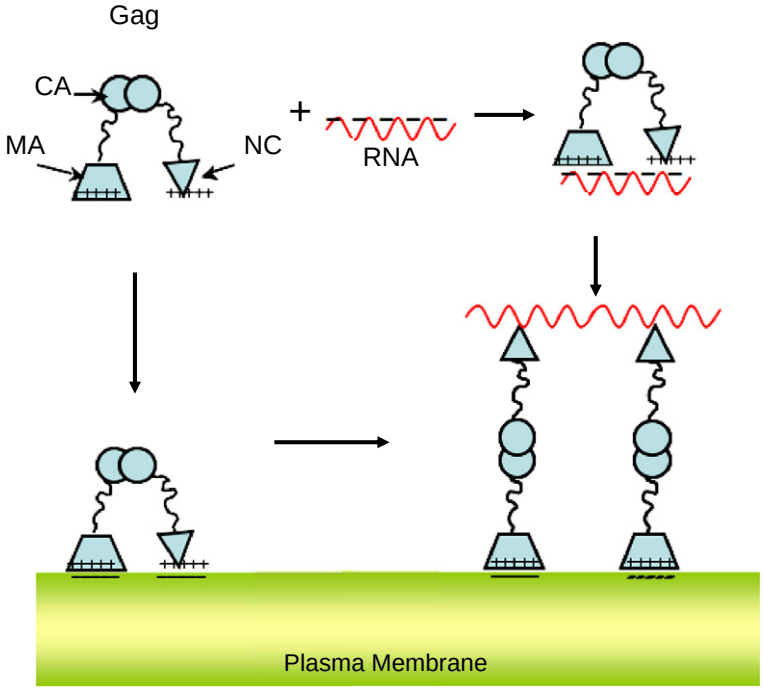

Fig. 4. A model for Gag extension consistent with structural characterization and known binding interactions of the protein. The Gag molecule is compact in solution, even when bound to RNA. RNA binds to the NC domain with very high affinity but evidently can also bind, with lower affinity, to the MA domain. The MA domain targets and anchors Gag to the anionic surface of the plasma membrane. Additionally, the NC domain may also associate with the membrane through electrostatic interactions. Only in the presence of all three components (protein, NA, and membrane) is extended Gag formed. A plausible mechanism is one in which the viral RNA and the membrane separate the terminal domains through their preferential interaction. Cross-linking several membrane-bound Gag molecules together by the RNA strand and interprotein interactions may further stabilize extended Gag.

viral membrane but lacks the full complexity of the HIV lipodome.[26] The Gag MA domain targets the membrane by a combination of electrostatic interactions originating from a patch of basic residues and hydrophobic interactions originating from an N-terminal myristate group thought to insert into the bilayer. However, the Gag construct in this study lacked the N-terminal myristate group and therefore relied on the contribution of electrostatic interactions to drive membrane binding. Earlier investigations have shown that, under certain conditions, electrostatics by itself is capable of orienting the MA domain in a manner consistent with proper viral assembly.[27]

A sequence of experiments outlined in Fig. 3a were conducted to investigate the structure of Gag protein on the model membrane. Initially, the neat, negatively charged bilayer was formed and measured by NR to ensure a defect-free, >90% complete membrane over the wafer surface. Gag was then introduced into the aqueous phase, where it bound to the membrane. The bound protein was then incubated with TGx7 to observe the effect of NA on the membrane-bound protein. Finally, the TGx7 construct was removed from the Gag molecules by flushing the sample cell with a high-salt (0.5 M NaCl) buffer.

Changes in the reflectivity spectra indicate both binding of Gag and modulation of protein conformation due to the different experimental conditions. Figure 3b shows the reflectivity profiles measured in the H_2O aqueous buffer contrast. Differences between the Gag protein conditions and the neat bilayer are shown as residuals in the bottom part of Fig. 3b. For each experimental condition, reflectivity spectra were measured using three separate isotopic aqueous buffer contrasts (pure H_2O, a 1:2 H_2O:D_2O mixture, and pure D_2O). The scattering from each contrast provides distinct reflectivity spectra, while the underlying protein and membrane structures are invariant. The reflectivity spectra from the additional buffer contrast conditions are provided in Supplementary Fig. 1.

Interpretation of the reflectivity profiles for these complex systems is only possible through the simultaneous fitting of a slab model to the complete set of reflectivity data. A "free-form" interpretation of the protein region (adjacent to outer leaflet headgroups) was used, wherein eight ≈ 30-Å slabs were allowed to vary independently. Hence, the best-fit nSLD profile is not based on any assumptions about protein structure. The nSLD profiles are shown in Fig. 3c where line widths are 95% confidence limits determined by Monte Carlo error analysis. A table of fit parameters used in the slab model that best fit the data and the parameter uncertainties are in Supplementary Table 1.

The nSLD profile for the neat bilayer is shown in Fig. 3c (black line) and indicates a nearly defect-free membrane, showing only bulk solvent after the

outer leaflet headgroup region. When Gag was introduced, it formed a protein layer with total dimensions of ≈90 Å (Fig. 3c, blue line). The subsequent introduction of single-stranded TGx7 DNA causes a shift in Gag dimension, extending to ≈190 Å (Fig. 3c, red line). These dimensions agree well with Gag protein dimensions in the immature virion.[4] A nearly complete recovery of the compact state of Gag was induced by the high salt rinse (Fig. 3c, green line). The insets showing Gag cartoon structures are illustrative models of possible protein conformations that are consistent with the overall dimensions determined by reflectivity. The SLD profile is likely an average of an ensemble of Gag conformations due to the intrinsically disordered regions between the structured domains. Protein extension was observed under conditions where 30% surface coverage by Gag was achieved. Through additional reflectivity measurements, we found that, below this minimal coverage on the tBLM, Gag protein remained folded (data not shown). Therefore, neighboring Gag–Gag interactions are apparently as important as Gag–membrane and Gag–NA interactions in contributing to the extension of the protein.

Our results show that on their own, protein–protein binding, protein–NA binding, or protein–membrane binding is not sufficient to trigger the rod-shaped conformation that Gag assumes in immature particles. However, simultaneously, all three binding interactions extend Gag to dimensions that are consistent with the immature virus particles. Based on the results reported here and the literature of binding interaction studied for the different Gag domains, a consistent model for how Gag conformations are modulated can be formed. This model is depicted schematically in Fig. 4.

A flexible Gag polyprotein, capable of adopting compact conformations with terminal MA and NC domains in close proximity, is a salient feature of the mechanism. The prevalence of positive charges on MA and NC domains allows them to interact simultaneously with polyanionic targets such as NAs or anionic membranes, maintaining the protein in compact conformation(s). Thus, compact Gag is observed in the presence of NAs only (Fig. 2) or membranes only (Fig. 3). However, in the presence of both membranes and NA, each of the domains binds its preferred target, allowing for extension of the protein—presumably mediated by Gag–Gag interactions. It should be noted that the composition of the membrane might influence this process *in vivo*.

In fact, a number of disparate observations are all in conformity with this picture. The N-terminal MA domain in Gag has been reported to associate with RNA likely through a patch of basic residues electrostatically attracted to the negatively charged RNA polymer.[28,29] Inositol pentakisphosphate (which resembles the anionic headgroups in the plasma membrane), together with NA, induces assembly of correctly sized VLPs.[9] Interestingly, both ends of the protein participate in stringent binding of IP6 in free solution;[6] footprinting shows that both domains can bind either RNA or phosphatidylinositol 4,5-bisphosphate (a plasma-membrane-specific phospholipid);[30] free MA as well as free NC can bind RNA;[31,32] and binding to RNA seems to modulate membrane interactions of Gag, contributing to the specific targeting of Gag to the plasma membrane.[31,33] Furthermore, the presence of the MA domain interferes with the ability of Gag to catalyze the annealing of tRNA to a complementary stretch in viral RNA, but this inhibition is relieved by IP6.[34]

It would appear from these results that HIV-1 Gag is incapable of proper particle assembly *in vivo* until it reaches the plasma membrane and is in contact with RNA. Further work is needed to dissect the temporal sequence of the events needed in Gag extension and subsequent assembly. Indeed, recent observations in live cells seem to indicate that the RNA genome is bound by a small number of HIV Gag molecules and targeted to the PM where more Gag molecules are recruited.[35] An understanding of virus assembly intermediates may suggest new leads for the development of therapeutics that inhibit proper virus formation.

Acknowledgements

This work utilized facilities supported in part by the National Science Foundation under Agreement No. DMR-0454672. This research was supported in part by the Intramural Research Program of the National Institutes of Health, National Cancer Institute, Center for Cancer Research.

Supplementary Data

Supplementary data to this article can be found online at doi:10.1016/j.jmb.2010.11.051

References

1. Swanstrom, R. & Wills, J. W. (1997). Synthesis, assembly, and processing of viral proteins. In *Retroviruses* (Coffin, J. M., Hughes, S. H. & Varmus, H. E., eds), pp. 263–334, Cold Spring Harbor Laboratory Press, Plainview, NY.
2. Ganser-Pornillos, B. K., Yeager, M. & Sundquist, W. I. (2008). The structural biology of HIV assembly. *Curr. Opin. Struct. Biol.* **18**, 203–217.

3. Zhou, W. J., Parent, L. J., Wills, J. W. & Resh, M. D. (1994). Identification of a membrane binding domain within the amino-terminal region of human immunodeficiency virus type 1 Gag protein which interacts with acidic phospholipids. *J. Virol.* **68**, 2556–2569.
4. Fuller, S. D., Wilk, T., Gowen, B. E., Kräusslich, H. G. & Vogt, V. M. (1997). Cryo-electron microscopy reveals ordered domains in the immature HIV-1 particle. *Curr. Biol.* **7**, 729–738.
5. Campbell, S. & Rein, A. (1999). In vitro assembly properties of human immunodeficiency virus type 1 Gag protein lacking the p6 domain. *J. Virol.* **73**, 2270–2279.
6. Datta, S. A. K., Zhao, Z., Clark, P. K., Tarasov, S., Alexandratos, J. N., Campbell, S. J. *et al.* (2007). Interactions between HIV-1 Gag molecules in solution: an inositol phosphate-mediated switch. *J. Mol. Biol.* **365**, 799–811.
7. Datta, S. A. K., Curtis, J., Ratcliff, W., Clark, P., Crist, R., Lebowitz, J. *et al.* (2007). Conformation of the HIV-1 Gag protein in solution. *J. Mol. Biol.* **365**, 812–824.
8. Byeon, I. J., Meng, X., Jung, J., Zhao, G., Yang, R., Ahn, J. *et al.* (2009). Structural convergence between cryo-EM and NMR reveals intersubunit interactions critical for HIV-1 capsid function. *Cell*, **139**, 780–790.
9. Campbell, S., Fisher, R. J., Towler, E. M., Fox, S., Issaq, H. J., Wolfe, T. *et al.* (2001). Modulation of HIV-like particle assembly in vitro by inositol phosphates. *Proc. Natl Acad. Sci. USA*, **98**, 10875–10979.
10. Tang, C., Ndassa, Y. & Summers, M. F. (2002). Structure of the N-terminal 283-residue fragment of the immature HIV-1 Gag polyprotein. *Nat. Struct. Biol.* **9**, 537–543.
11. Gamble, T. R., Yoo, S. H., Vajdos, F. F., von Schwedler, U. K., Worthylake, D. K., Wang, H. *et al.* (1997). Structure of the carboxyl-terminal dimerization domain of the HIV-1 capsid protein. *Science*, **278**, 849–853.
12. De Guzman, R. N., Wu, Z. R., Stalling, C. C., Pappalardo, L., Borer, P. N. & Summers, M. F. (1998). Structure of the HIV-1 nucleocapsid protein bound to the SL3 Psi-RNA recognition element. *Science*, **279**, 384–388.
13. Lee, B. M., De Guzman, R. N., Turner, B. G., Tjandra, N. & Summers, M. F. (1998). Dynamical behavior of the HIV-1 nucleocapsid protein. *J. Mol. Biol.* **279**, 633–649.
14. Newman, J. L., Butcher, E. W., Patel, D. T., Mikhaylenko, Y. & Summers, M. F. (2004). Flexibility in the P2 domain of the HIV-1 Gag polyprotein. *Protein Sci.* **13**, 2101–2107.
15. Stys, D., Blaha, I. & Strop, P. (1993). Structural and functional studies *in vitro* on the p6 protein from the HIV-1 *gag* open reading frame. *Biochim. Biophys. Acta*, **1182**, 157–161.
16. Curtis, J. E., Raghunandan, S., Nanda, H. & Krueger, S. (2010). *SASSIE: A program to study intrinsically disordered biological molecules and macromolecular ensembles using experimental scattering restraints.* http://www.smallangles.net/sassie/SASSIE/SASSIE_HOME.html.
17. Campbell, S. & Vogt, V. M. (1997). In vitro assembly of virus-like particles with Rous sarcoma virus Gag deletion mutants: identification of the p10 domain as a morphological determinant in the formation of spherical particles. *J. Virol.* **71**, 4425–4435.
18. Yu, F., Joshi, S. M., Ma, Y. M., Kingston, R. L., Simon, M. N. & Vogt, V. M. (2001). Characterization of Rous sarcoma virus Gag particles assembled in vitro. *J. Virol.* **75**, 2753–2764.
19. Fisher, R. J., Fivash, M. J., Stephen, A. G., Hagan, N. A., Shenoy, S. R., Medaglia, M. V. *et al.* (2006). Complex interactions of HIV-1 nucleocapsid protein with oligonucleotides. *Nucleic Acids Res.* **34**, 472–484.
20. McGillivray, D. J., Valincius, G., Vanderah, D. J., FeboAyala, W., Woodward, J. T., Heinrich, F. *et al.* (2007). Molecular-scale structural and functional characterization of sparsely tethered bilayer lipid membranes. *Biointerphases*, **2**, 21–33.
21. Cornell, B. A., Braach-Maksvytis, V. L. B., King, L. G., Osman, P. D. J., Raguse, B., Wieczorek, L. & Pace, R. J. (1997). A biosensor that uses ion-channel switches. *Nature*, **387**, 580–583.
22. Shenoy, S., Moldovan, R., Fitzpatrick, J., Vanderah, D. J., Deserno, M. & Loesche, M. (2010). In-plane homogeneity and lipid dynamics in tethered bilayer lipid membranes (tBLMs). *Soft Matter*, **6**, 1263–1274.
23. Parratt, L. G. (1954). Surface studies of solids by total reflection of x-rays. *Phys. Rev.* **95**, 359–369.
24. Heinrich, F., Ng, T., Vanderah, D. J., Shekhar, P., Mihailescu, M., Nanda, H. & Lösche, M. (2009). A new lipid anchor for sparsely-tethered bilayer lipid membranes. *Langmuir*, **25**, 4219–4229.
25. Kienzle, P. A., Doucet, M., McGillivray, D. J., O'Donovan, K. V., Berk, N. F. & Majkrzak, C. F. (2000). *ga_refl*, a program for simultaneous fitting of X ray and neutron polarized reflectometry data; http://www.ncnr.nist.gov/reflpak.
26. Brügger, B., Glass, B., Haberkant, P., Leibrecht, I., Wieland, F. T. & Kräusslich, H. G. (2006). The HIV lipidome: a raft with an unusual composition. *Proc. Natl Acad. Sci. USA*, **103**, 2641–2646.
27. Nanda, H., Datta, S. A. K., Heinrich, F., Lösche, M., Rein, A., Krueger, S. & Curtis, J. E. (2010). Electrostatic interactions and binding orientation of HIV-1 matrix, studied by neutron reflectivity. *Biophys. J.* **99**, 2516–2524.
28. Purohit, P., Dupont, S., Stevenson, M. & Green, M. R. (2001). Sequence-specific interaction between HIV-1 matrix protein and viral genomic RNA revealed by in vitro genetic selection. *RNA*, **7**, 576–584.
29. Hearps, A., Wagstaff, K. M., Piller, S. C. & Jans, D. (2008). The N-terminal basic domain of the HIV-1 matrix protein does not contain a conventional nuclear localization sequence but is required for DNA binding and protein self-association. *Biochemistry*, **47**, 2199–2210.
30. Shkriabai, N., Datta, S. A. K., Zhao, Z. J., Hess, S., Rein, A. & Kvaratskhelia, M. (2006). Interactions of HIV-1 Gag with assembly cofactors. *Biochemistry*, **45**, 4077–4083.
31. Alfadhli, A., Still, A. & Barklis, E. (2009). Analysis of human immunodeficiency virus type 1 matrix binding to membranes and nucleic acids. *J. Virol.* **83**, 12196–12203.
32. Lochrie, M. A., Waugh, S., Pratt, D. G., Clever, J., Parslow, T. G. & Polisky, B. (1997). In vitro selection of RNAs that bind to the human immunodeficiency virus type-1 gag polyprotein. *Nucleic Acids Res.* **25**, 2902–2910.

33. Chukkapalli, V., Oh, S. J. & Ono, A. (2010). Opposing mechanisms involving RNA and lipids regulate HIV-1 Gag membrane binding through the highly basic region of the matrix domain. *Proc. Natl Acad. Sci. USA*, **107**, 1600–1605.
34. Jones, C. P., Datta, S. A. K., Rein, A., Rouzina, I. & Musier-Forsyth, K. (2010). Matrix domain modulates HIV-1 Gag's nucleic acid chaperone activity via inositol phosphate binding. *J. Virol.* In press. doi:10.1128/JVI.01809-10.
35. Jouvenet, N., Simon, S. M. & Bieniasz, P. D. (2009). Imaging the interaction of HIV-1 genomes and Gag during assembly of individual viral particles. *Proc. Natl Acad. Sci. USA*, **106**, 19114–19119.